minerals

MDPI

Article

Multi-Analytical Techniques to Define the Mineralogical and Petrophysical Characteristics and Provenance of Siliceous Lithic Findings: The Case Study of La Calvera Rock Shelter (Cantabria, Spain)

Stefano Columbu [1], Dario Fancello [1,*], Gianni Gallello [2], Mirco Ramacciotti [2] and Agustin Diez-Castillo [2]

[1] Dipartimento di Scienze Chimiche e Geologiche, University of Cagliari, Cittadella Universitaria di Monserrato, Monserrato, 09042 Cagliari, Italy
[2] Department of Prehistory, Archaeology and Ancient History, University of Valencia Av. Blasco Ibáñez, 28, 46010 Valencia, Spain
* Correspondence: dario.fancello@unica.it; Tel.: +39-0706757712

Abstract: This archaeometric study aims at characterizing the archaeological finds belonging to the lithic industry from La Calvera rock shelter (Camaleño, Cantabria) and at hypothesizing the possible provenance of each material. The site, located in the mountainous area of Picos de Europa National Park (more than 1000 m a.s.l.) close to the megalithic complex of Peña Oviedo, is characterized by the presence of hearths and charcoal remains, ancient pottery, and a rich lithic assemblage composed of siliceous rocks dating back to >8000 BP and linked to the first Holocene occupations of the Cantabrian Mountains. For the study of the rock shelter's lithic assemblage, a multi-analytical approach was used: SEM-EDS and XRD analyses were performed to define the microtextural characteristics of samples and to identify the amorphous/crystalline phases; physical and mechanical tests were conducted to define the petrophysical properties (density, porosity, imbibition and saturation indexes, mechanical strength) of the samples. Preliminary data of chemical compositions, obtained by portable XRF, are also presented. The results show that the different siliceous materials (quartzite, cherts, hyaline quartz) can be distinguished through the basic analytical techniques used here. In addition, most of the archaeological samples have mineralogical and petrographic features similar to the natural samples coming from nearby outcrops, corroborating the hypothesis of a local material supply. The presence of local sources of useful raw materials could have favoured the site's occupation. Finally, the diverse compositional and textural feature of the analysed materials result in different mechanical properties (porosity, density, hardness, workability), so they likely had different uses and technical functions.

Keywords: chert; chunk; rock crystal; siliceous findings; prehistoric; SEM-EDS; XRD; porosity; density; petrophysical; mechanical

Citation: Columbu, S.; Fancello, D.; Gallello, G.; Ramacciotti, M.; Diez-Castillo, A. Multi-Analytical Techniques to Define the Mineralogical and Petrophysical Characteristics and Provenance of Siliceous Lithic Findings: The Case Study of La Calvera Rock Shelter (Cantabria, Spain). *Minerals* **2023**, *13*, 666. https://doi.org/10.3390/min13050666

Academic Editor: Alberto De Bonis

Received: 1 March 2023
Revised: 24 April 2023
Accepted: 9 May 2023
Published: 12 May 2023

1. Introduction and Aims

A rock shelter is an opening of modest size and extension that is generally formed by weathering and erosion processes (e.g., induced by water run-off) of a rock that is less resistant than the surrounding rocks. Shelters are horizontally shallow, unlike caves generated by karstification, which are much deeper. Rock shelters can have an archaeological importance since they were often used by humans as refuge from the weather [1–4]. Prehistoric people frequented such shelters as a place to live, leaving behind tools and other artefacts that now assume a high archaeological significance [5–8].

La Calvera rock shelter is located in Picos de Europa National Park, 1180 m above sea level, close to Camaleño (Cantabria; Figure 1), in the area of the Peña de Oviedo megalithic complex. From the geologic point of view, the Picos de Europa is an imposing mountain

range within the Cordillera Cantabrica (Figure 1), with a geological history linked to the Variscan and Alpine orogeneses. The Peña de Oviedo area, where the Calvera rock shelter site is located, is mainly characterized by Palaeozoic lithologies, such as limestone, quartzite, sandstone and shales, and subordinate Quaternary deposits (Figure 1).

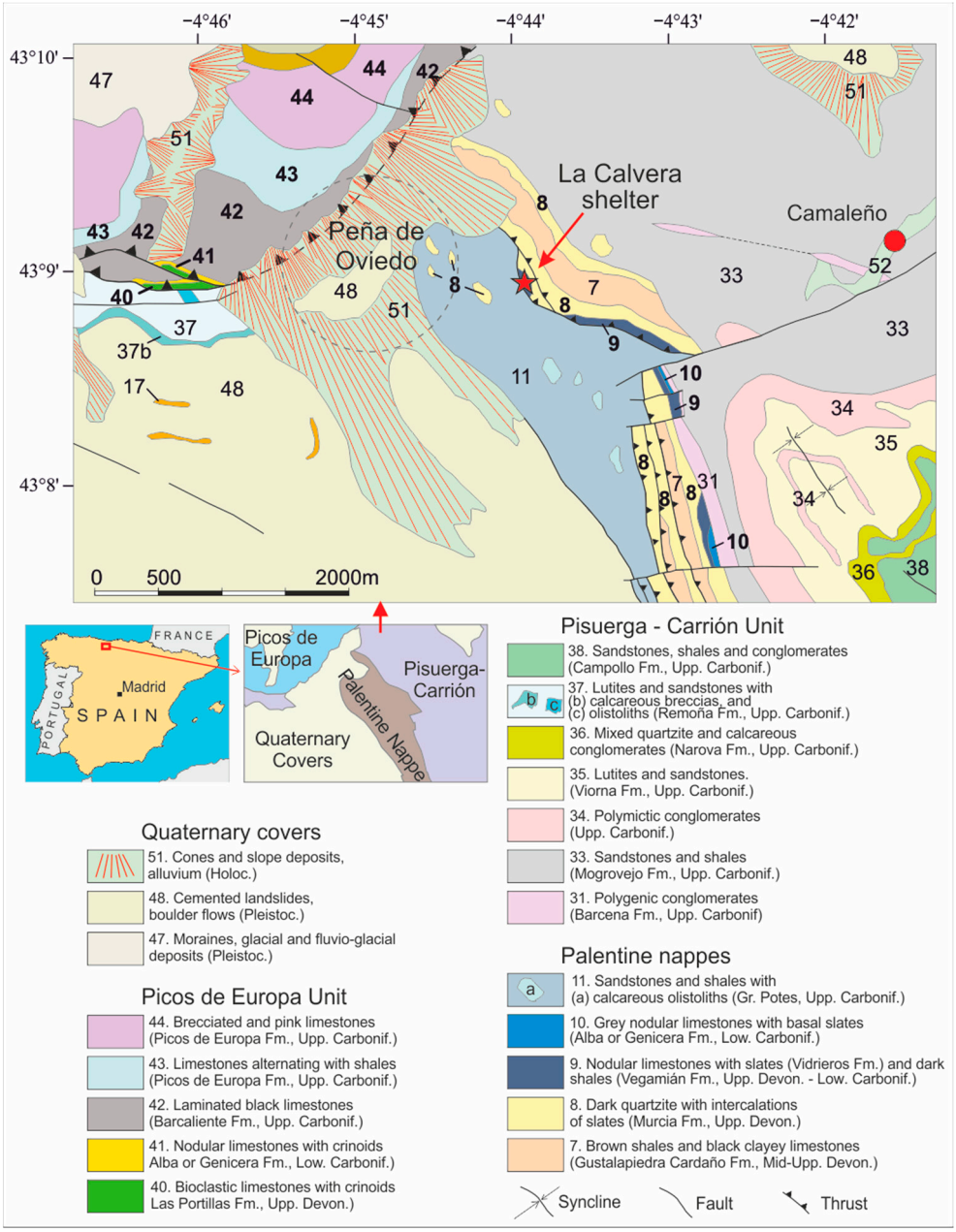

Figure 1. Geological map of the Peña de Oviedo sector (west territory of Camaleño village) at scale 1:50.000 from Sheet 81—Potes modified, Instituto Geològico y Minero de España web site at link: http://info.igme.es/cartografiadigital/geologica/Magna50Hoja.aspx?language=es&id=81 (accessed on 15 March 2023). The inlets show the position of the study area in Spain (red rectangle) and a sketch map of the tectonic units in which the area is subdivided. The numbers of the formations are taken from the original map (sheet 81—Potes); those in bold indicate the formation hosting cherts and/or quartzites.

During the excavations in the La Calvera rock shelter, the archaeologists documented the presence of hearths and charcoal, historical pottery in the upper levels, and the presence of a lithic assemblage composed of different siliceous rocks (chert, rock crystal, quartzite)

dating back to >8000 BP and linked to the first Holocene occupations of the Cantabrian Mountains [9]. More than 500 lithic fragments were discovered with some retouched pieces (mainly cores, scrapers and small blades).

Chert is a very fine-grained siliceous rock composed almost exclusively of microcrystalline quartz and chalcedony. It is normally found in the form of layers or as nodules and lenses within carbonate rocks or alternated with clay-rich shale levels. Stratified cherts are essentially of biogenic origin and owe their formation to the accumulation of the siliceous shell or skeleton organisms (e.g., radiolarians, diatoms, silico-flagellates and sponges) [10], even if recent studies suggest a significant role of diagenesis in silica redistribution in bedded cherts [11]. Nodular cherts generally have a diagenetic origin and would form as a result of silicification processes inside the host rocks [10]. The contribution of hydrothermal fluids interacting with seawater in the depositional environment has been reported locally by several authors [12,13]. Given their high hardness, chemical and physical resistance, conchoidal fracturing and its use as fire starter, this material had an important use in the ancient lithic industry, especially in prehistoric times. On the basis of the different chipping techniques of cherts, subperiods and, thus, the working material culture of civilizations can be identified.

Contrary to chert, the term quartzite is more ambiguous since historically it has been used with different meanings to describe a wide variety of rocks of both metamorphic and sedimentary origin [14]. Moreover, distinguishing among different types of quartzite is often not easy due to the similar mineralogy and textures that different quartzites can share. As recently pointed out by Prieto et al. [15] the full characterization of this material should be achieved through a detailed petrographic analysis integrated with digital imaging to recognize and quantify the textural features of quartz grains; however, this kind of approach is necessarily destructive and, thus, cannot be applied to highly valuable archaeological finds. In this paper, the term quartzite is used to refer to silicified quartzarenites (also known as orthoquartzite) almost completely composed of quartz. The discrimination between quartzite and cherts has been performed through macroscopic and microscopic observation (under reflected light), following the criteria proposed by [14] and concerning the fracturing, the luster, the grain size of the samples.

The provenance and lithic supply in Cultural Heritage studies [16,17] are fundamental to define the dynamics involving human populations and their surrounding environment, mobility, and possible relations among different settlements; however, matching prehistoric artefacts and raw materials from potential quarries just on the basis of naked-eye examination is often controversial. Only a multidisciplinary approach, based on the use of different analytical techniques, allows for the full characterization of the archaeological geomaterials and their natural counterparts [17–22], leading to more objective and robust results [23–25].

The study of the lithic assemblage from La Calvera rock shelter, has been performed through a two-stage, multi-analytical approach. Firstly, a large set of samples was analysed using non-destructive to micro-destructive techniques, based on smartphone imaging and molecular spectroscopy techniques [26], to understand if it is possible to distinguish siliceous materials coming from different source areas and finally to identify the supply area of archaeological finds. Secondly, according to the first analyses, a subset of samples was selected to carry out a petrographic, mineralogical and petrophysical characterization (this study). This second stage is aimed at further characterizing the selected samples and to test the hypothesis postulated after the former analyses. To achieve this goal, the microstructural and textural features of both the amorphous and crystalline phases within the samples were observed through a scanning electron microscope (SEM-EDS) and analysed by powder X-ray diffraction (XRD) to detect minor phases and the degree of crystallinity. Finally, the physical and mechanical characteristics were determined to understand the technical properties of the artefacts in relation to their possible use as tools. A summary of the chemical composition of the different lithotypes is also reported.

2. Geological Setting and Natural Chert Occurrences

The Cordillera Cantabrica extends for about 480 km along the northern Spain coast, from Galicia (to the west) to Basque Country (to the east). The Picos de Europa area, where the La Calvera rock shelter is located (close to the Camaleño area, Figure 1), is in the central part of the Cordillera. The current relief of the Cantabrian zone is the result of the superposition of the Variscan and Alpine orogeneses during the Palaeozoic and Cainozoic Eras, respectively [27,28]. The orogenic cycles led to the stacking of different tectonic units that mostly share the same sequence of lithostratigraphic formations, even if a local variability is observed. Indeed, from one unit to another, the same formation could have, or could even lack, different features and different thickness. Additionally, the name of the same formation can change depending on the unit or on the locality in which it occurs [29].

The area of Peña de Oviedo, where the La Calvera shelter rests, is located on the south-eastern side of the Picos de Europa park, close to the Camaleño village (Figure 1). In this area, only the Picos de Europa Unit (northwest) and the Pisuerga-Carrión Unit (south-east) were cropped out, separated by a regional thrust. The former is characterized by a predominance of upper Carboniferous limestone [30] belonging to the formations of Picos de Europa and Barcaliente (previously known as Caliza de montaña). Small slices of limestones belonging to the Las Portillas and Alba (or Genicera) Fm., also occur in the southern side of the Barcaliente Fm. The Pisuerga-Carrión Unit consists of several formations (Barcena, Viorna, Narova, Remoña and Campollo Fms.), mainly siliciclastic (slates, shales, sandstone and conglomerates) with limestone intercalation, of the Carboniferous age [31]. A sequence of allochthonous Devonian to Carboniferous rocks covers large areas of the Pisuerga-Carrión Unit; this sequence, referred to as Palentine Nappes or Palentian domain [32] consists of alternating siliciclastic and calcareous deposits grouped in different formations. From the bottom to the top, they are the Gustalapiedra Cardaño Fm., Murcia Fm, Vidrieros Fm., Vegamian Fm., Alba Fm., and finally the Carboniferous sequence of the Potes group.

Quaternary covers consist of moraines, glacial/fluvio-glacial deposits, cemented landslides and boulder flows from the Pleistocene, and torrential cones, slope deposits and alluvium from the Holocene [33,34]. It was during this period, dominated by important glacial systems of the Cantabrian Mountains and interglacial stages [35–37], that the Picos de Europa area assumed its current physiognomy and the typical rock shelters developed, mainly in the calcareous lithologies.

Several authors investigated the outcropping formations in the Cantabrian region to identify the potential sources of the lithic artefacts found in prehistoric human settlements [29,38,39]. In particular, Herrero-Alonso et al. [29] compiled an updated and complete inventory of the chert-bearing formations in a wide area of the Cantabrian region that includes the study area of this paper. According to these authors, in the surroundings of Peña de Oviedo, cherts, radiolarites and/or quartzite of knappable quality can be found in the Las Portillas, Barcaliente and Picos de Europa formations (all belonging to the Picos de Europa unit) and in the Vegamián formation (Palentine Nappe). The Alba (or Genicera) formation, also hosting knappable cherts, is found in both units forming decametre-thick slices. Quartzite occurrences in the surroundings of La Calvera have been reported in the Murcia Fm. [40] and in the Vidrieros Fm. [41], associated with chert nodules. None of the cited quartzites have a metamorphic origin, rather, they are the result of sedimentary/diagenetic processes. Chert-bearing formations are documented also in some areas of the Pisuerga-Carrión Unit, but they do not occur in the study area. The features of these cherts and the comparison with the archaeological finds of La Calvera will be outlined in the Section 5.

3. Materials and Methods

Based on the spectroscopic analyses and colour features on a large sample set, ten representative samples were selected and analysed in this work (Table 1, Figure 2). One

cobble of macrocrystal quartz or rock crystal (AR10), three samples of local grey chert (flakes: AR12.1 and AR18.2, chunk: RM03.4), one sample of ochre chert (AR21), two samples of quartzite (AR29 and AR34) and one sample of yellowish chert (AR37). Finally, for comparison with macroscopically similar chert, two samples of Domeño chert collected from the geological outcrop of Andilla (Valencia, Spain) were also analysed.

Table 1. Analysed samples (artefacts and chunk raw materials) from La Calvera rock shelter and geological samples from the Domeño area in Andilla (Valencia, Spain).

Sample	Rock type	Classification	Origin
AR10	Rock crystal	Chunk	La Calvera rock shelter
AR12.1	Grey chert	Flake	La Calvera rock shelter
AR18.2	Grey chert	Flake	La Calvera rock shelter
AR21	Ochre chert	Flake	La Calvera rock shelter
AR29	Quartzite	Flake	La Calvera rock shelter
AR34	Quartzite	Flake	La Calvera rock shelter
AR37	Yellow chert	Chunk	La Calvera rock shelter
RM03.4	Grey chert	Chunk	La Calvera rock shelter
AN1.2	Domeño chert	Outcrop sample	Andilla (Valencia)
AN5.1	Domeño chert	Outcrop sample	Andilla (Valencia)

Each sample was cleaned with deionized water and a brush in order to remove superficial contaminations and incrustations prior to the analyses.

A small chip of each sample was powdered to carry out XRD analyses, which were performed at the Department of Chemical and Geological Sciences (University of Cagliari). XRD patterns were acquired by a PANalytical X'Pert Pro diffractometer (Malvern PANalytical, Almelo, The Netherlands) that works with theta-theta geometry using Ni-filtered Cu Kα1 radiation (λ = 1.540598 Å) and equipped with a X'Celerator detector. Operative conditions were acquisition range 5–70°, step size 0.008°, 0.19 s per step, voltage 40 kV and current 40 mA. Data were processed by X'Pert HighScore Plus (TM) 2.1.2 software using the PDF2 database (released in 2010 by ICDD, Newtown Square, PA, USA).

SEM analyses were performed on ten samples using a Quanta Fei 200 equipped with a ThermoFischer Ultradry EDS detector, at the CeSAR laboratories (University of Cagliari, Italy). Raw samples were put into the sample chamber without conductive coating to preserve them for further analyses, thus, low-vacuum conditions (0.3 to 0.5 torr) were used to dissipate electrons from incident beam. Variable spot sizes of 4–5 (in arbitrary units given by the Quanta Fei equipment) and an accelerating voltage of 15–25 kV were adopted during the analytical sessions.

Petrophysical and mechanical tests on the samples were performed on ten specimens of the most significant samples. Physical tests were carried out according to Buosi et al. [42] and Columbu et al. [43,44] (see the Supplementary SM1).

Multielement analysis was performed on a larger sample set, including ten chunks of grey chert used as raw materials, twenty-four fragments of the same grey chert, six cherts of different types, fifteen fragments of quartzite, six rock crystal fragments and eleven fragments of Domeño chert. Elemental concentrations of Al, K, Ca, Fe, Ti and Zr were detected using a S1 Titan portable energy dispersive X-ray fluorescence spectrometer (pXRF) equipped with a Rh X-ray tube (50 kV) and X-Flash® silicon drift detector (Bruker, Billerica, MA, USA). Internal calibration Geochem-trace was used. Each sample was analysed between two and up to five spots, and the results were then averaged.

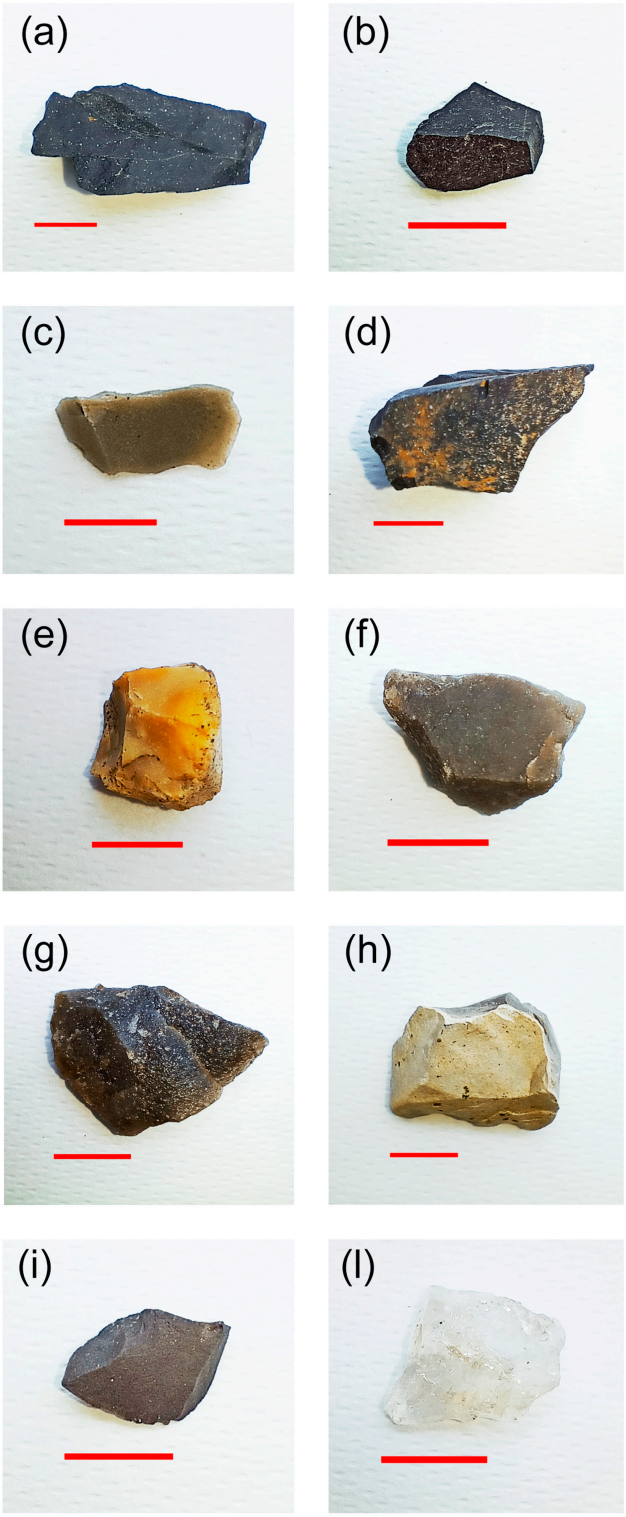

Figure 2. Main representative samples of cherts, rock crystals and chunk raw materials analysed from La Calvera rock shelter: (**a**) grey chert of AR12.1 sample; (**b**) grey chert of AR18.2 sample; (**c**) grey-ochre chert of AR21; (**d**) raw material chunk of RM3.4 sample; (**e**) yellow chert of AR37 sample; (**f**,**g**) quartzite of AR29 and AR34 samples; (**h**,**i**) Domeño cherts of AN5.1 and AN1.2 samples (from Andilla, Valencia); (**l**) rock-crystal of AR10 sample. Red line is 1 cm.

4. Results

4.1. Compositional Characteristics

The characterization of mineralogical and amorphous (or with low crystallinity) phases and microtextural features was performed on 10 major samples considered most significant of the facies studied. After studying the macro- mesoscopic characteristics by optical microscopy analysis in reflected light (Table 2), the samples were analysed using scanning electron microscopy (SEM-EDS) and X-ray diffractometry (XRD). The results, reported in the next two paragraphs, allow for a preliminary comparison between the archaeological and geological samples in terms of characteristic compositional aspects aimed at the study of material provenance from the rock outcrops.

Table 2. Macroscopic characteristics of archaeological finds and geological samples by optical microscopy in reflect light.

Sample	Classification	Description
AR10	Rock crystal	Colourless hyaline quartz with yellowish hues
AR12.1	Grey chert	Blackish surface with shiny appearance, compact but very rich in micro-grain alterations giving a porous appearance
AR18.2	Grey chert	Blackish with shiny appearance, compact with micro-grain alterations (similar to sample AR12.1)
AR21	Grey-ochre chert	Grey-beige, compact with conchoid-type fracturing and with porous appearance
AR29	Dark quartzite	Presence of dark-to-light colour gradient in thickness: dark side more porous and altered, light side shiny as formed by microcrystals (similar to sample AN5.1)
AR34	Dark quartzite	Dark in colour, porous and altered (similar to the dark side of sample ARCH29 but shinier)
AR37	Yellowish chert	Yellow-brown colour, with varied surface appearance: from smooth and firm in some places, to extremely porous in others
RM03.4	Grey chert	Black colour, shiny, almost obsidian-like appearance, with conchoid fractures, rich in alterations and also in diffuse patina (similar to sample 12.1)
AN1.2	Blackish chert	Blackish colour, compact with conchoid fracturing, low porosity, clean surface (no soil residue on the surface)
AN5.1	Grey-beige chert	Grey-beige surface with no soil residue on the surface, porous but compact appearance with conchoid-type fracturing

4.1.1. SEM-EDS Analysis

The results are reported in Table 3. Back scattered electrons (BSE) imaging at low magnifications (about 100×) shows that most samples look similar, with a dark-grey surface disseminated with light-grey spots, particles, and/or undefined stains (Figure 3a,b). Higher magnifications (400–800×) reveal that the surface is commonly quite irregular due to the presence of micrometre-sized cracks, holes and euhedral microcrystals (Figure 3c,d). Exceptions to this general appearance are the samples AR10 (rock crystal, Figure 3e), and AR34, whose surface is more compact and homogeneous.

Table 3. Microscopic and mineralogical characteristics of archaeological finds and geological samples using SEM-EDS analyses.

Sample	Classif.	Textural/Structural Description	Qtz	Si-Al	Cal	Fe-ox	Ti-ox	Notes	Grain-Size Frequency Range (μm)	
AR10	Rock crystal	Extremely compact, conchoid fractures, common Si-Al micro-grains, Fe oxide, gypsum, Zn oxide, Sn and P-REE, presence of NaCl surface patina	X	X		X	X	Zn oxide, Sn, Gyp, P-REE, NaCl	25	120
AR12.1	Grey chert	Cribrous and rough appearance with microcavities filled by alteration phases, abundant metal oxides	X	X *		X	X	Zircons; Fe, Ni, Cr oxides	8	50
AR18.2	Grey chert	Cribrous, rough appearance with microcavities filled by alteration phases, with many diffuse oxides	X	X	X	X	X	Gypsum and abundant Ti	5	30
AR21	Grey-ochre chert	Compact homogeneous surface, with diffuse niches rich in Si-Al phases and few metal oxides	X	X			X	/	1	12
AR29	Dark quartzite	Partly compact and clean and partly covered with earthy sediment, with scattering of Si-Al phases and metal oxides	X	X		X	X	P-REE	10	80
AR34	Dark quartzite	Partly compact and clean and partly covered with earthy sediment, with scattering of Si-Al phases, metal oxides and P-REE	X	X		X	X	P-REE, Zircon, phyllosilicate	30	150
AR37	Yellowish chert	Cribrous or locally smooth surface with scantily scattered light spots (without the presence of oxides or Si-Al phases)	X	X		Traces		/	8	20
RM03.4	Grey chert	Cribrous, rough appearance resulting from the presence of oxide patinas, with portions of the surface clean and smooth, unaltered quartz	X	X		XX	X	/	10	40
AN1.2	Blackish chert	Compact appearance but appearing earthy at medium magnifications, covered with microparticles, and scattered with oxides of Fe, Ti and framboids	X	X	X	X	X	Pyrite framboids	3	15
AN5.1	Grey-beige chert	Compact appearance but earthy at medium magnifications, covered with microparticles, scattered with oxides of Fe, Ti and Cr	X	X	X	X	X	Fe-Cr grains and Ni oxides	2	10

Legend: X = presence of phases; XX = abundant; / = not detected; * = Si-Al phases with peaks of various other elements (mainly Na, K, Ca, Fe, Mg). P-REE = REE phosphates.

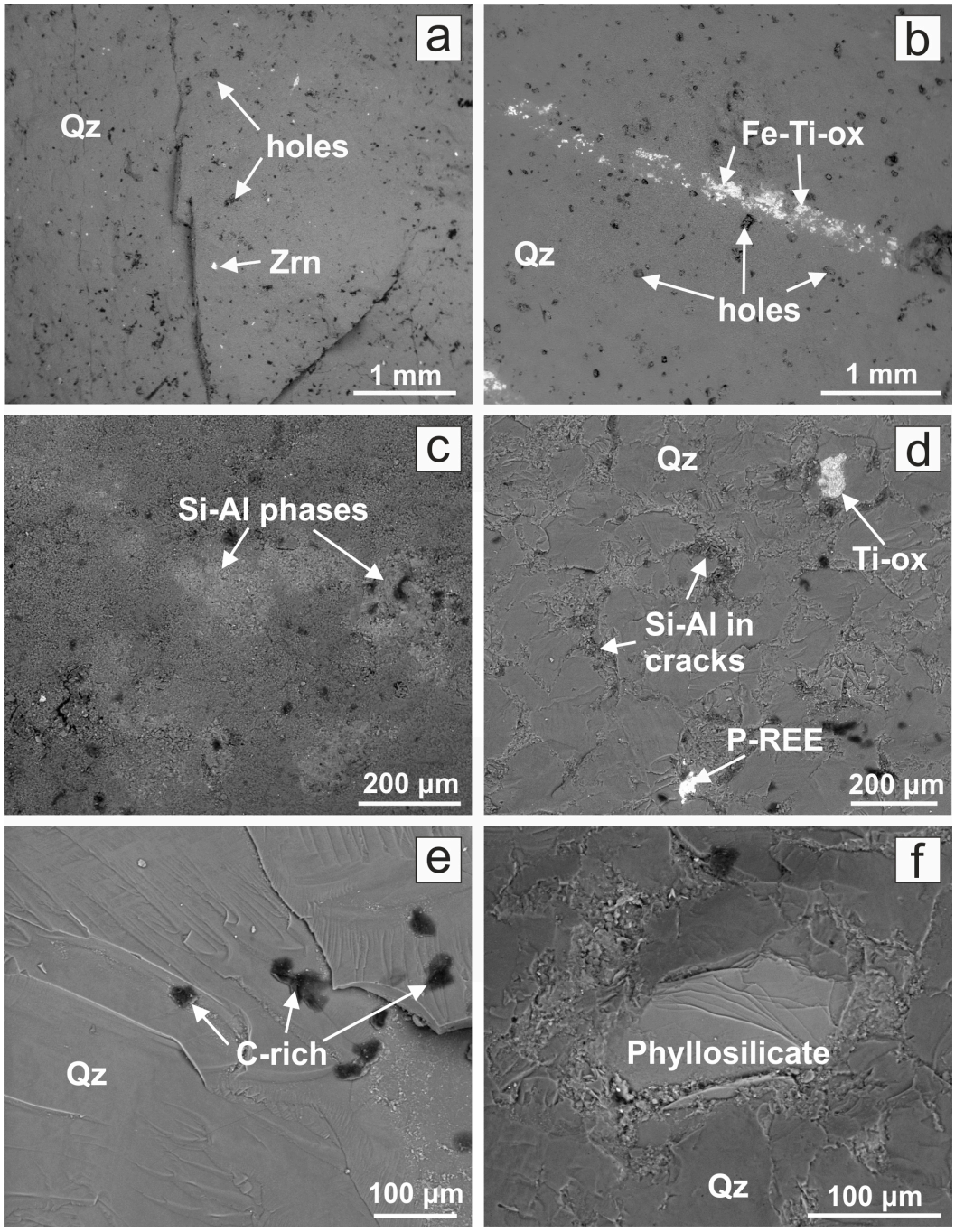

Figure 3. BSE images representative of analysed samples: (**a**) AR12.1 (grey chert) at low magnification, showing an apparent compact texture with cracks, holes (sometimes filled by phyllosilicates) and bright spots of zircon and metal oxides; (**b**) millimetres-long trail of Fe and Ti oxides within the quartz matrix (AN5.1,Grey-beige chert from Domeño); (**c**) AR37 (yellow chert) at moderate magnification that shows the rough surface covered by small crystals and plagues of light-grey phyllosilicates; (**d**) quartz matrix of AR29 (dark quartzite) hosting a REE-phosphate grain and Ti oxide; (**e**) compact and homogeneous surface of AR10 (rock crystal) samples with dark-grey stains due to carbon (organic?) impurities; (**f**) phyllosilicate in quartz matrix (AR34).

Energy dispersive spectroscopy (EDS) analyses, even if just qualitative, provide evidence of the different phases in each sample. The most common phases (other than quartz) are represented by Si-Al-bearing (±K, Ca, Na, Fe, Mg) minerals in form of fine-grained alteration patinas (Figure 3c,d) or having a phyllosilicate-like, tabular habitus

(Figure 3f). Fe and/or Ti oxides are also widespread and were found in all samples in variable amounts and occurrences (isolated crystals, aggregates, oriented trails, patinas, etc.) (Figure 3a,d and 4a,b). Other minor phases are calcite (Figure 4c,d), whose former presence is testified also by euhedral holes (Figure 4d,e), gypsum (AR10, AR18.2, not shown) and pyrite in framboidal aggregates (AN1.2) (Figure 4c). Traces of Ni-Cr oxides, zircon fragments and REE-phosphates were locally observed (Figure 3a,d and Figure 4a). Characteristic snowflake-like patinas of NaCl have been observed only in sample AR10 (Figure 4f).

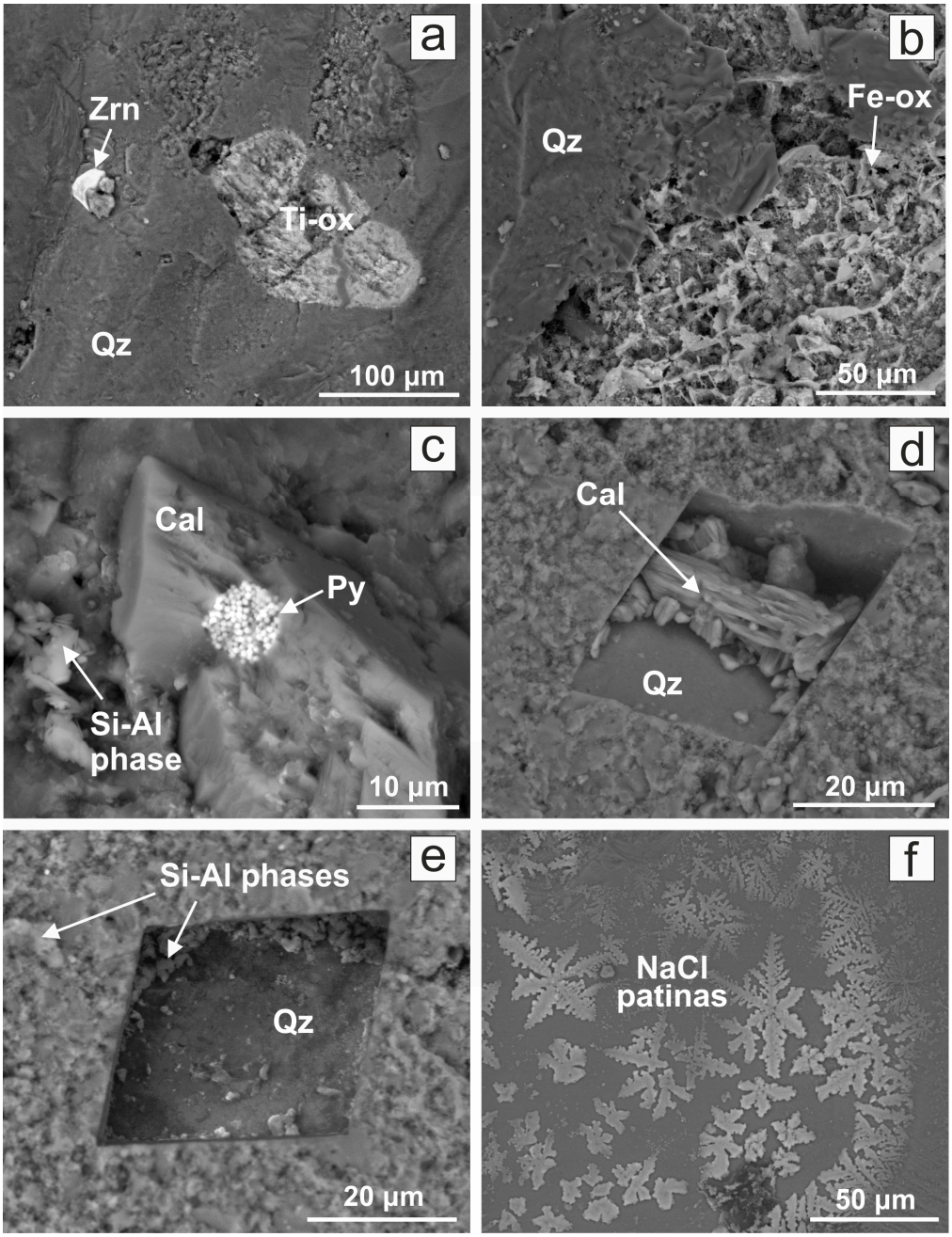

Figure 4. BSE images representative of analysed samples: (**a**) corroded crystal of Ti-oxide and zircon in AR18.2 (grey chert); (**b**) Fe-oxide encrustation on the surface of the sample RM3.4 (grey chert); (**c**) framboidal pyrite on a calcite crystal at high magnification (AN1.2, blackish chert, Domeño); (**d**) negative crystal shape on the AN5.1 (grey-beige chert, Domeño) surface, formerly hosting calcite, whose remains are still preserved; (**e**) negative crystal shape of calcite, now totally removed; (**f**) NaCl patinas with particular snowflake-like habitus on the AR10 (rock crystal) surface.

Looking at Table 3, which reports a summary of the phases detected by the SEM analyses, the discrimination between the different categories of lithic fragments appears quite hard. Generally, a higher abundance of metal oxides, especially Fe, Ti and Zn, has been observed in greyish cherts and in RM3.4 whose surface was largely covered by reddish oxides encrustation (Figure 4b). Oxides seems to be less abundant in quartzite samples, even in the yellowish samples. The two samples from Andilla have very diffuse calcite crystals likely linked to the geology of the surrounding rocks. Despite these differences, samples belonging to different categories can host the same phases, and samples of the same type can have different phases; in other words, there are no minerals diagnostic of a given type. This is likely due to the samples' heterogeneity but also to the fact that SEM imaging investigates small areas, so it cannot be considered statistically representative of the whole sample.

4.1.2. XRD Analysis

The mineralogical composition and a synoptic scheme of all XRD patterns are reported in Table 4 and in Figure 5, respectively. To highlight the minor peaks, the Y-axes (counts) have been reported in square root. Furthermore, to facilitate the pattern comparison, all Y-axes were set to a maximum value of 70,000 counts.

Table 4. Mineralogy of archaeological finds and geological samples by XRD analysis.

Sample	Type	Classification	Main Minerals			Minor or Accessory Minerals				Crystallinity
			α-Qtz	Cal	Ant	Phyl	Py	Rt	Dol	%
AR10	Archaeological find (artefact)	Rock crystal	X							100
AR12.1	Archaeological find (artefact)	Grey chert	X		X	X	X			84
AR18.2	Archaeological find (artefact)	Grey chert	X		X	X	X		X	88.5
AR21	Archaeological find (artefact)	Grey-ochre chert	X	(X)						61.6
AR29	Archaeological find (artefact)	Dark quartzite	X							99
AR34	Archaeological find (artefact)	Dark quartzite	X			X		(X)		95
AR37	Archaeological find (artefact)	Yellowish chert	X							80
RM03.4	Raw material (chunk)	Grey chert	X							86
AN1.2	Geological sample	Blackish chert	X	X						65.3
AN5.1	Geological sample	Grey-beige chert	X	(X)	X					84

X = phase identified; (X) = doubtful identification by XRD but supported by SEM-EDS analysis.

All samples exhibit the typical patterns of well crystalline quartz that, using the "search and match" tool of X'Pert HighScore Plus software, provide a score of 75%–85% with synthetic quartz (Ref. code 00-046-1045 in PDF database). Despite the similarity of all samples, a difference can be observed: samples AR10, AR29 and AR34 show a higher crystallinity compared to the other samples. Indeed, they show higher intensities and lower FWHM (full width at half maximum) of all peaks, and those that are more evident are positioned at about 20.87°, 50.13° and 59.95° 2θ angles. This means that quartzite samples are almost as crystalline as the pure rock crystal.

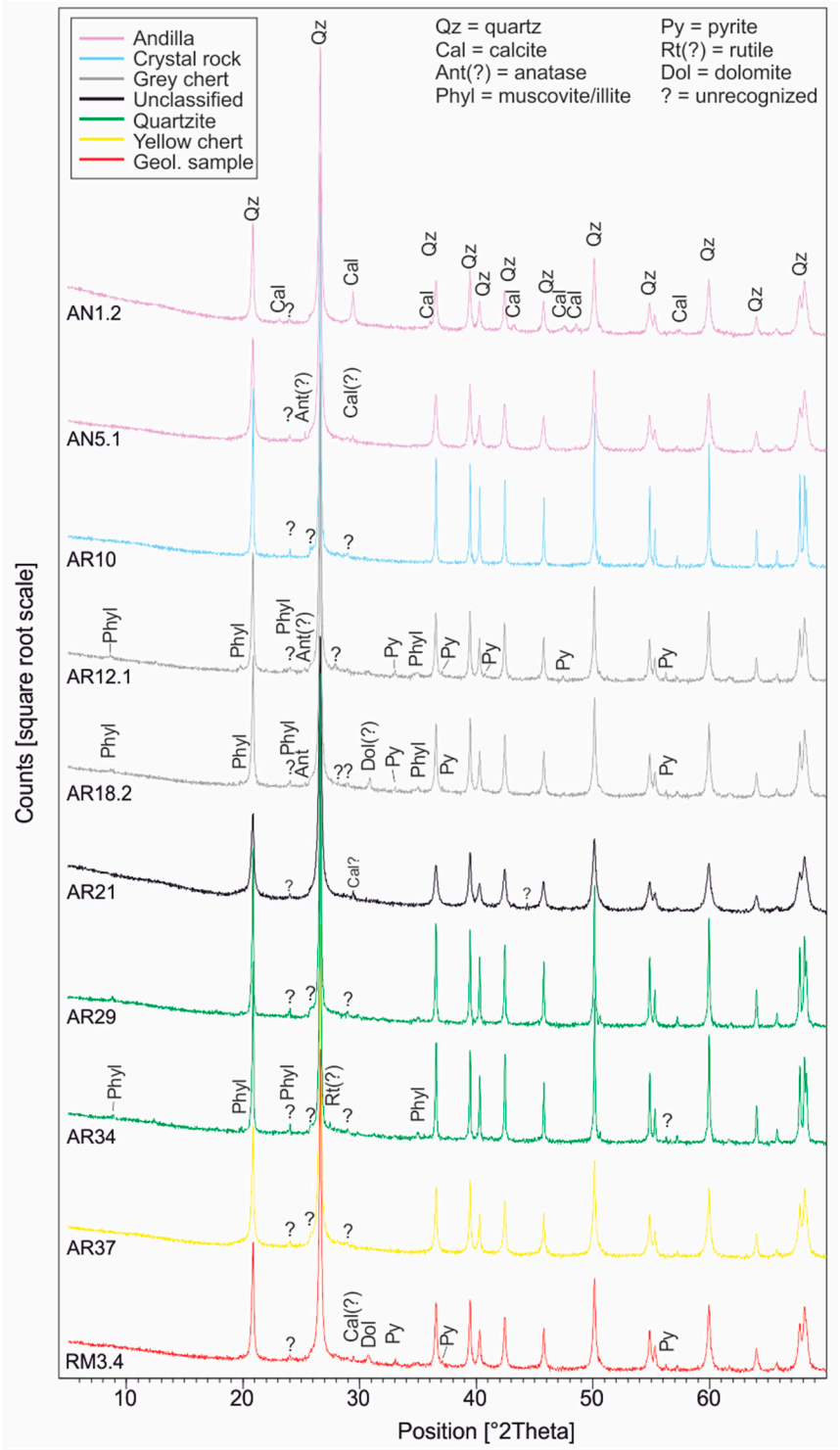

Figure 5. XRD patterns of the selected samples of cherts (AR12.1, AR18.2, AR21, AR29, AR34, AR37), rock crystal (AR10), raw material (RM03.4) and geological samples (AN1.2, AN5.1). Abbreviations followed by question marks corresponds to phases for which a clear assignment was not possible (see text).

The measurement of the crystallinity degree (reported in Table 4) has been performed comparing the background signals of each sample with the background of a reference material of known crystallinity. The AR10 crystal rock was chosen as a reference material of almost perfect crystallinity, assigning it the value of 100%. The results of this calculation method should be carefully considered since it works when comparing similar samples

(i) whose only difference is in the crystallinity degree and (ii) that are measured using the same operative conditions. In this case, the second requirement is met, whereas the first is only partially met since samples slightly differ from each other due to the presence of minor phases. To lessen the effect produced by other phases, only the region of the XRD pattern ranging from 19° to 23° 2θ, where the {100} quartz peak occurs at 20.86° 2θ, was considered. This calculation confirms the higher crystallinity of quartzite samples AR29 and AR34 (99% and 95%, respectively, Table 4). Greyish AR12.1 and AR18.2 and yellowish AR37 cherts share a similar crystallinity of 84%, 88% and 80%, respectively. Andilla cherts have crystallinity of 84%, so they are highly comparable with local and archaeological cherts. Significantly lower values are found in the grey-ochre chert AR21 = 62% (Table 4).

The matrix crystallinity shows a general positive correlation (R^2 = 0.68, Figure 6) with the particle grain size obtained by SEM analysis. We can observe three populations of samples with different behaviours due to the diverse petrogenesis of these siliceous rocks, especially regarding the crystal rock and the quartzite samples with respect to the cherts.

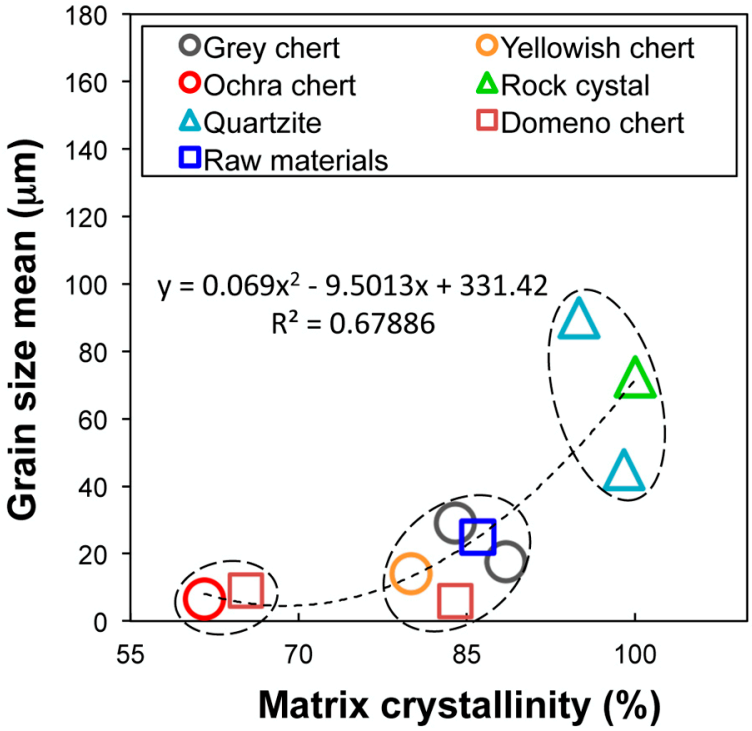

Figure 6. Positive correlation between the matrix crystallinity determined by comparing of the background signals of each sample with the background of a reference known crystallinity of the AR10 crystal rock and the grain size means determined by SEM analysis (see Table 3).

The identification of minor phases is quite difficult since the intense signal of quartz peaks hides the contribution of minor phases, and also because the latter are present in very low amounts. Thus, in many cases, only the main peak of the minor phases can be observed, and it is not possible to assess the presence of a phase with certainty just by one or two peaks. However, by comparing the patterns of all samples and by coupling these pieces of information with those of the SEM analyses, it is possible to identify some phases with good reliability, whereas some other can be just hypothesized. Calcite is clearly identified in sample AN1.2 by the detection of its six higher peaks; the most intense one, at 29.40° 2θ, has been also found in AN5.1, AR21 and RM3.4 and, even if it is the only peak ascribable to calcite in these samples, its presence is reliable since it is supported by the SEM-EDS analyses. The presence of a ferroan dolomite/ankerite can be supposed in AR18.2 and RM3.4, which show a peak at 30.94° 2θ angle, but this is the only evidence of this mineral; therefore, it is too weak to clearly assess its presence. Pyrite has been identified by five peaks in AR12.1, and three of them have been found in AR18.2 and RM3.4. Interestingly,

the only sample where pyrite was identified by SEM analysis (AN1.2) does not show peaks referrable to it. An undefined phyllosilicate phase (illite/muscovite) has been recognized in AR12.1, AR18.2 and AR34 through the identification of very small peaks at about 8.8°, 19.8° and 34.9° 2θ angles; this is a tentative association since the maximum peak of these phyllosilicates (at about 26.6°) is hidden by the strongest quartz peak; however, the finding of tabular Si-Al-phases by SEM-EDS suggests the correctness of this assumption. Another plausible phase, identified by XRD analyses, is a Ti oxide that could be either anatase or rutile; these minerals share a similar position of the strongest peak at about 25.3° 2θ but this is the only visible peak (in AN5.1, AR12.1 and AR18.2) that can be assigned to this phase. However, the presence of a Ti-oxide, as well as the phyllosilicate phase, is supported by SEM-EDS observation and analyses (Figures 4 and 5; Table 3). The sample AR34 does not show the anatase/brookite peak but is the only sample that has an unassigned peak at 27.4° 2θ and that is compatible with the strongest peak of rutile (another Ti oxide polymorph). Different unassigned peaks are found in all patterns the most noticeable of which are those at 25.3° and 29.0° 2θ that recur in almost all patterns. Other unassigned peaks are found locally at 25.8° 2θ (in four samples) and at 56.3° 2θ only in AR34. Despite its ubiquitous presence, Fe oxides were not detected by XRD, probably due to their low crystallinity. Likewise, the other accessory minerals identified by SEM (zircon, P-REE, gypsum, etc.) were not detected due to their very low content.

4.2. Petrophysical Properties

For a complete characterization of the analysed archaeological and geological samples, and to understand the technical properties of the artefacts, the following main petrophysical properties were determined: real density, bulk density, open porosity to helium, open and closed porosity to water, imbibition coefficient (expressed in weight), saturation index, punching resistance index, and the compressive and tensile strengths calculated indirectly (Table 5). The physical and mechanical properties are variously affected by different compositional features of the samples. Figure 7 shows the graphs that plot the data (Table 5) of the main physical properties that have been determined. In Figure 7a, which shows the open porosity to helium against the bulk density, a high variability (Table 5) of the open porosity (i.e., interconnected) is observed, which is mainly induced by the compositional heterogeneity and only subordinately by the decay of the samples.

Table 5. Petrophysical and mechanical properties of archaeological and geological samples.

Sample	Origin	Type		ρ_R (g/cm^3)	ρ_B (g/cm^3)	Φ_O He (%)	Φ_O H_2O (%)	IC_W (%)	SI (%)	$Is_{(50)}$ (MPa)	R_C (MPa)	R_T (MPa)
AR21	Artefact	Grey-ochre chert	Group 1	2.56	2.41	5.9	5.3	2.2	89.8	9.8	195.2	7.8
AN1.2	Geolog. samples from Domeño (Andilla)	Blackish chert		2.54	2.41	5.1	2.5	1.0	49.2	15.2	303.1	12.1
AN5.1		Grey-beige chert		2.52	2.38	5.8	5.6	2.3	96.6	8.0	160.1	6.4
AR12.1	Artefact	Grey chert	Group 2	2.65	2.59	2.1	1.8	0.7	85.8	8.6	171.6	6.9
AR18.2	Artefact	Grey chert		2.63	2.56	2.9	2.8	1.1	97.2	11.5	230.3	9.2
AR37	Artefact	Yellowish Chert		2.58	2.50	3.2	3.1	1.3	96.7	7.0	140.5	5.6
AR10	Artefact	Rock-crystal		2.64	2.61	1.2	1.0	0.4	83.5	4.9	99.0	4.0
AR29	Artefact	Dark quartzite		2.65	2.61	1.8	1.7	0.6	96.8	15.3	306.9	12.3
AR34	Artefact	Dark quartzite		2.65	2.62	1.2	1.2	0.5	97.6	8.3	165.5	6.6
RM03.4	Raw material (chunk)	Grey chert		2.65	2.58	2.7	1.4	0.6	52.7	7.5	149.6	6.0

Legend: ρ_R = real density; ρ_B = bulk density; Φ_O He = helium open porosity; Φ_O H_2O = water open porosity; IC_W = imbibition coefficient; SI = saturation index; $Is_{(50)}$ = point load test strength index; R_C = indirect calculated compression strength; R_T = indirect calculated tensile strength.

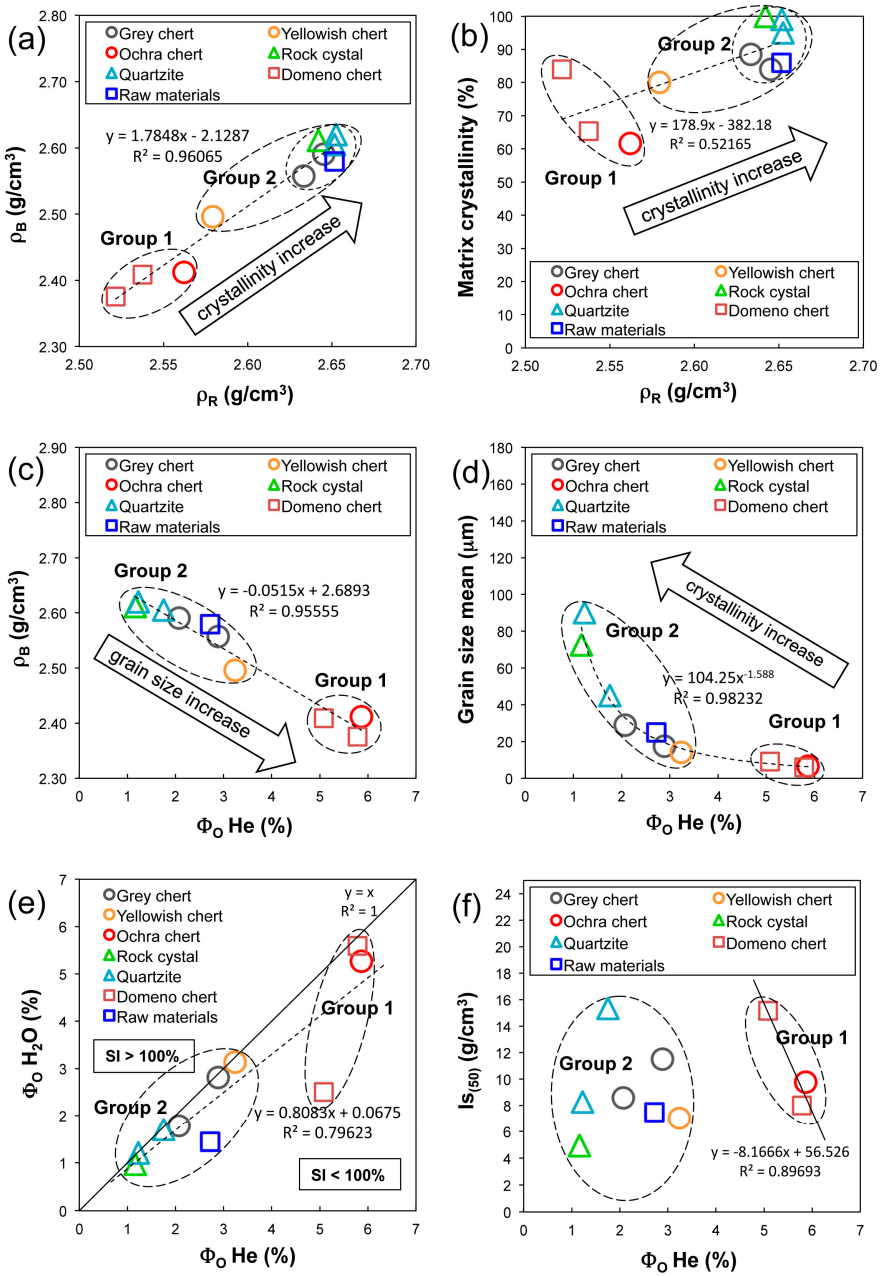

Figure 7. Petrophysical and mechanical properties of archaeological and geological samples: (**a**) real density vs. bulk density; (**b**) real density vs. matrix crystallinity; (**c**) open helium porosity vs. bulk density; (**d**) helium open porosity vs. phase size mean; (**e**) helium open porosity vs. water open porosity; (**f**) open helium porosity vs. PLT punching strength index.

The real density, related to the characteristics of the solid phases (mineralogical and amorphous), reflects the compositional differences. The samples of Domeño cherts (AN01.2, AN05.1 from the Andilla area) and grey-ochre chert (AR21), which have similar values ranging from 2.52 to 2.56 g/cm^3 for real density and from 2.38 to 2.41 g/cm^3 for bulk density, belong to the first homogeneous group (Figure 7a), while the remaining samples (i.e., AR12.1, AR18.2, AR37, AR10, AR29, AR34, RM03.4) constitute a second homogeneous group, in which sample AR37 also falls, which, however, shows intermediate behaviour between the two groups (Figure 7a). Given that the real density of the amorphous phases is lower (about 2.3–2.55 g/cm^3) than the crystalline phases of α-quartz (2.65 g/cm^3), a light positive correlation (R^2 = 0.52) between the real density and the degree of matrix crystallinity is observed (Figure 7b).

The open porosity to helium, ranging from 5.1% to 5.9% in Group 1 and from 1.2 to 3.2% in Group 2 (Table 5), affects the bulk density, as shown in Figure 7c, with a high correlation coefficient (R^2 = 0.96). The porosity of these samples is mainly represented by intraphase pores with planar geometry; thus, it shows a positive correlation with the size of the amorphous/crystalline phases (Figure 7d) with a high correlation coefficient (R^2 = 0.98). The water open porosity shows a trend similar to that of helium open porosity. Additionally, it shows lower values ranging from 2.5% to 5.6% in Group 1 and from 1.0 to 3.1% in Group 2 (Table 5, Figure 7e). The saturation index (graphically shown in Figure 7e) shows values that are always lower than 100% and generally range from 85% to 98% (Table 5), except two samples (i.e., Domeño chert AN01.2 and raw material RM03.4) belonging to the first and second sample groups, respectively, which have lower values (i.e., 49% and 53%, Table 5).

Regarding the physical and mechanical properties, the samples show a great dispersion of data with high standard deviations (Table 5). The first group shows values of the PLT punching strength index from 8 to 15.2 MPa, while the Group 2 shows values ranging from 4.9 to 15.3 MPa (Table 5, Figure 7d).

Contrary to what is commonly reported in the literature, the strength index does not show a clear negative correlation with porosity (Figure 7f), probably due to the very low porosity values with small differences between samples. Only within Group 1 does a clear link between the two inversely proportional properties become evident.

In addition to porosity, the mechanical strength is also variously and subordinately influenced by the grain size of the phases (see Figure 8a), the degree of crystallinity of the matrix (see Figure 8b), and in some cases, by the presence of anisotropy (i.e., samples AR12.1, RN3.4) or crystal (i.e., sample AR10) planes that weaken the microstructure from a physical and mechanical point of view.

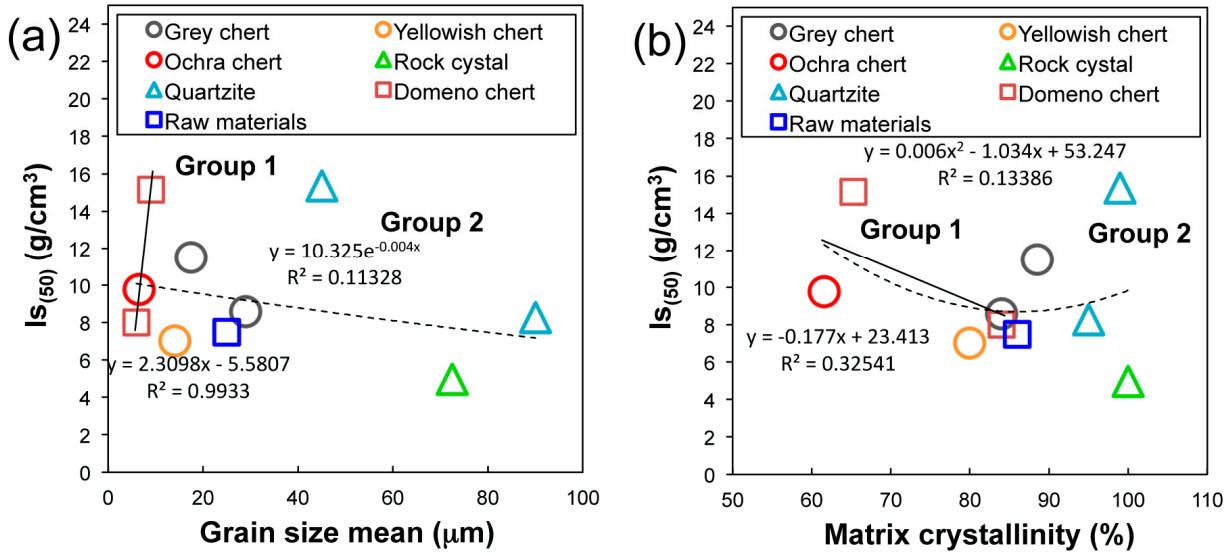

Figure 8. Petrophysical and mechanical properties of archaeological and geological samples: (**a**) phase size mean vs. PLT punching strength index; (**b**) matrix crystallinity vs. PLT punching strength index.

4.3. Preliminary Results of Multielement Analysis

The average elemental concentrations and standard deviation for the different classes of samples are shown in Table 6.

Table 6. Average elemental concentrations of the different classes of samples obtained by pXRF.

Class		Al	K	Ca	Ti	Fe	Zr
Raw material chunks	Mean	0.88	0.21	0.05	0.066	0.33	59
(*n* = 10)	SD	0.23	0.05	0.05	0.014	0.08	22
Grey chert	Mean	1.15	0.26	0.035	0.06	0.30	55
(*n* = 24)	SD	0.55	0.16	0.019	0.02	0.14	30
Other cherts	Mean	0.38	0.045	0.03	0.008	0.07	<LD
(*n* = 6)	SD	0.08	0.019	0.02	0.002	0.05	
Quartzite	Mean	1.5	0.28	0.045	0.09	0.5	185
(*n* = 15)	SD	0.7	0.14	0.019	0.04	0.6	115
Rock crystal	Mean	<LD	0.022	0.023	0.020	0.053	<LD
(*n* = 6)	SD		0.007	0.009	0.007	0.013	
Domeño chert	Mean	0.30	0.07	1.9	0.016	0.16	9
(*n* = 11)	SD	0.05	0.02	1.1	0.004	0.02	2

Note: Elemental concentrations are expressed as mass percentage, except for Zr, which are expressed as mg/kg. <LD: below the limits of detections; *n* = number of samples; SD: standard deviation.

As can be observed in Figure 9, grey chert flakes and chunks have similar levels for all the analysed elements, suggesting that the former were probably obtained from the latter as raw material. On the other hand, the other chert types show lower concentrations for Al, K, Ti, Fe and Zr. Domeño chert has the highest amounts of Ca. Average concentrations of quartzite are higher than those of cherts for most elements. Quartzite samples also have a higher variance.

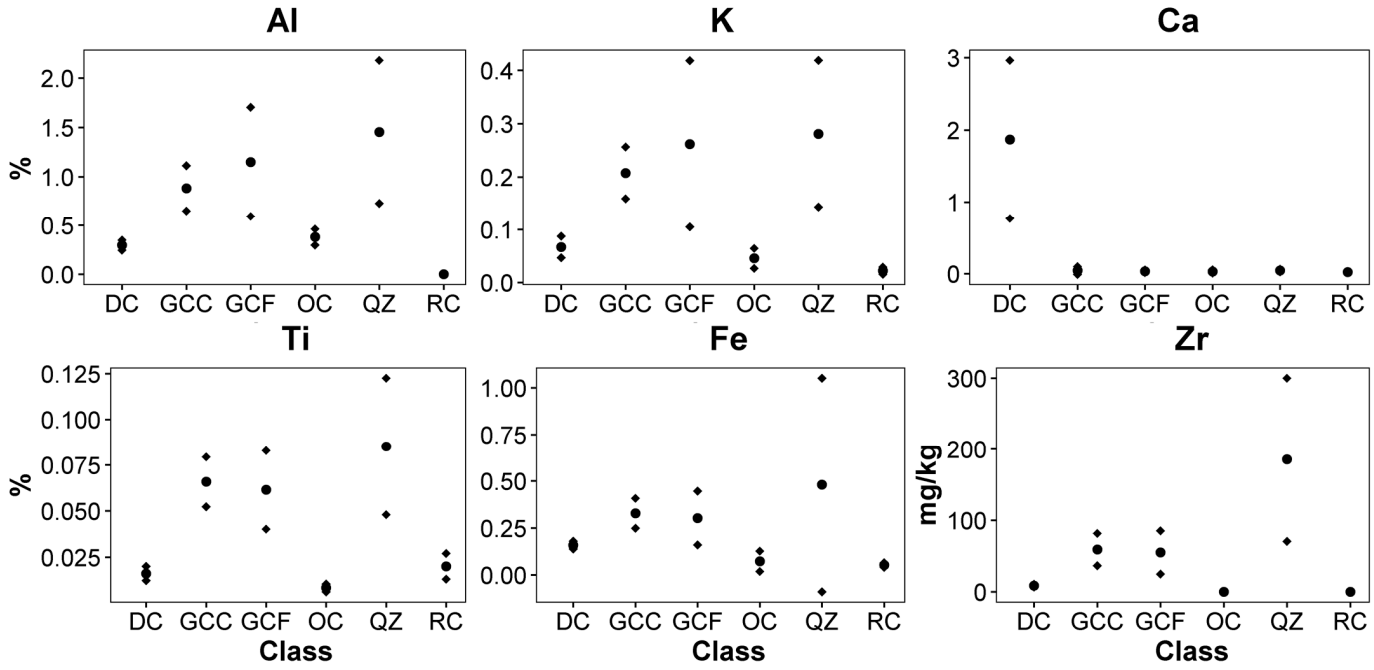

Figure 9. Mean (●) and standard deviation (⧫) of the elemental concentrations for the six classes of samples (DC: Domeño chert; GCC: grey chert chunks; GCF: grey chert fragments; OC: other cherts; QZ: quartzite; RC: rock crystal).

5. Discussion

The investigations performed on the archaeological and geological samples yielded significant results regarding the sourcing, use and compositional characteristics of siliceous findings and raw materials coming from the area surrounding the La Calvera rock shelter archaeological site.

First, the petrographic and mineralogical investigations have allowed for the classification of the studied archaeological samples, mainly as cherts and subordinately as quartzites and "rock-crystals". The mineralogical analyses by XRD on the lithic finds have revealed both higher crystallinity and grain size in the quartzite and crystal rock samples in comparison with cherts. The different crystallinity and grain size have also been confirmed by the petrophysical analysis. In detail: the real density to which it is positively correlated, while the porosity of rocks shows a negative correlation, confirms the presence of intraparticle planar pores among the particles (grains). The physical tests highlight the presence of two main different behaviours of the samples: the first population consisting of the archaeological cherts, quartzites and chunks of raw materials coming from the Calvera rock shelter, and a second subordinate sample population consisting of Domeño cherts from Andilla and the unclassified grey-ochre chert. Mechanical strength is high and comparable in the different samples analysed, due to the low overall porosity of the materials, which does not exceed 5%; however, the lower grain size and crystallinity of the chert microstructure, characterised by a more "brittle" physical and mechanical behaviour with pseudo-conchoidal microfracturing, probably facilitates the processing and production of sharper edges than quartzites and crystal rocks. The lithic assemblage of La Calvera shows that chert artefacts are commonly smaller than quartzite ones, likely due to different uses, which, in turn, are influenced by different petrophysical properties. The higher flakeability of cherts resulted in its suitability for arrowheads and cutting tools, whereas the coarser, less porous (<3%), and denser (>2.6 g/cm3) quartzites produced thicker and heavier tools, such as pestles or scrapers.

The measurement of the physical properties performed in this study was also aimed at testing the effectiveness of this approach in distinguishing among the different materials and, in future studies, using this information to identify potential sources. The data obtained seem to be inconclusive, but it must be considered that they are just preliminary results and that the method needs a wider sample set to be tested and statistically validated. From the available data, it can be observed that the foreign samples of Domeño, introduced to test the method, show a distinct behaviour in all diagrams of Figure 7 and can be grouped together with ochre cherts. Yellowish cherts have physical features between those of the Domeño and La Calvera materials. Considering that the analysed samples display detectable differences in their petrophysical properties, even if similar from a mineralogical point of view, we believe this approach is worth being tested further.

SEM-EDS allowed for the definition of the microstructural and textural characteristics of samples, highlighting specific discriminant compositional information on single samples by the identification of minor or accessory phases, e.g., the relatively high content of calcite, distinctive of Andilla Domeño cherts and also confirmed by XRD results. However, a clear signature of each specific source (or material) cannot be found by SEM-EDS and/or XRD analyses since it would require detailed partially destructive investigation on every lithic fragment.

Based on the above-described analyses, some provenance hypothesis can be made.

The excavation campaigns at La Calvera rock shelter discovered abundant chunks and cores of grey chert (samples AN01.2, AN05.1, A12.1, AR18.2) from different archaeological levels, making this lithic material the most representative of the site. Considering these abundant findings and the proximity of La Calvera to chert-bearing rocks [29,41], a local supply of this grey chert can be reasonably hypothesized.

Grey and black cherts are also commonly found within the Cantabrian Range but only the Alba Fm. (Lower Carboniferous), Barcaliente Fm. (previously known as Caliza de Montaña, Mountain Limestone, Upper Carboniferous) and Picos de Europa Fm. (Upper Carboniferous) are locally present [29]. In addition, a report of greyish chert associated with dark quartzites is described by Castillo-Diez [41] within the Vidrieros Fm., in close proximity to the shelter of La Calvera, and in contact with the quartzites of the Murcia Fm. Although it is difficult to distinguish between the aforementioned cherts based on of the obtained results, the presence of some mineralogical peculiarities detected by XRD and SEM-

EDS (i.e., presence of phyllosilicates, massive texture, absence of fossils, negligible amounts of Ca and Mg), would lean toward the Barcaliente Fm. cherts [29] or to the Vidrieros/Murcia Fms. The latter can be identified just by its proximity and by the macroscopic description since no analytical data can be found in the literature. On the other hand, we cannot exclude that further outcrops of the same chert, nor that cherts and quartzite boulders of secondary origin (i.e., from colluvial or alluvial deposits), were exploited [40].

As regards the yellow chert (AR37), petrographic and mineralogical data corroborate the first identification with a Piloña chert outcropping, based on chemical and macroscopic features, in eastern Asturias about 50 km NW of the studied site [38,45]. This chert circulated in the area and is present in other Mesolithic sites of the area [46]. The performed analyses pointed out the difference between the grey-ochre chert artefact (AR21) and local chert, suggesting a different and possibly non-local provenance. Concerning quartzite samples, little information is available in the literature ([40] and references therein), but a local source is the most plausible assumption since dark quartzite occurs in the Vidrieros Fm. [41] and in the Murcia Fm [40]. Rock crystal, as well, is possibly local [46], but a precise identification of the source area cannot be established.

6. Conclusions

The multidisciplinary research gave interesting results for the characterisation of siliceous rock artefacts and the raw materials provenance study, confirming the support of the non-destructive SEM analyses.

The petrographic and mineralogical characterisation carried out on a subset of samples previously analysed by colour analysis and other spectroscopic techniques allowed for the definition of the provenance of the different siliceous rocks, especially for cherts. According to the analytical results, most of the archaeological chert samples have chemical characteristics compatible with natural ones outcropping in the same area, confirming the close supply, which could have possibly favoured the occupation of the site. As regards the origin of the quartzite from the territory, the previous studies do not provide enough information, and samples from geological outcrops should be added to obtain more robust data. Rock crystal samples probably have a local raw material supply, because quartz crystals are commonly found in Mesolithic contexts in the southern areas of the Picos de Europa Fm. and in eastern Asturias.

The study of the physical and mechanical properties has been proved to be a new and very fruitful approach in the characterization of cherts because it can provide useful information on the different mechanical behaviours of siliceous samples, which certainly conditioned the workability and, thus, the uses, technical functions and production of tools of antiquity. The lower crystallinity of cherts affects its flakeability and the typical conchoidal fracturing, resulting in sharp tools suitable for arrowheads and small cutting tools. Quartzite, which is coarser, less porous and denser, was used to produce larger tools such as beating masses and scrapers.

Supplementary Materials: The following supporting information can be downloaded at: https://www.mdpi.com/article/10.3390/min13050666/s1, SM1: methods and formulas for the determination of the petrophysical properties.

Author Contributions: Conceptualization, S.C.; methodology, S.C. and D.F.; validation, S.C., D.F., G.G. and M.R.; formal analysis, S.C. and D.F.; investigation, S.C. and G.G.; data curation, S.C. and D.F.; writing—original draft preparation, S.C.; writing—review and editing, S.C., D.F., G.G. and M.R.; visualization, S.C., D.F., G.G., M.R. and A.D.-C.; supervision, S.C.; project administration, S.C. All authors have read and agreed to the published version of the manuscript.

Funding: This research was funded by the Ministry of Education, Culture and Sport of the Valencian Government for the "Smartphone and Green Analytical Chemistry" project (PROMETEO 2019-056).

Acknowledgments: Stefano Columbu and Dario Fancello acknowledges the CeSAR Laboratory of Cagliari University for the SEM analyses. Gianni Gallello acknowledges the financial support of the Beatriz Galindo Fellowship (2018) funded by the Spanish Ministry of Science and Innovation and Ministry of Universities (Project BEAGAL18/00110 "Development of analytical methods applied to archaeology"), and of Mirco Ramacciotti of the "Margarita Salas" fellowship (MS21-176) funded by the Ministry of Universities of Spain. Three anonymous reviewers are acknowledged for the great improvement brought to the manuscript.

Conflicts of Interest: The authors declare no conflict of interest.

References

1. Fullagar, R.L.K.; Price, D.M.; Head, L.M. Early Human Occupation of Northern Australia: Archaeology and Thermoluminescence Dating of Jinmium Rock-Shelter, Northern Territory. *Antiquity* **1996**, *70*, 751–773. [CrossRef]
2. Robbins, L.H.; Murphy, M.L.; Brook, G.A.; Ivester, A.H.; Campbell, A.C.; Klein, R.G.; Milo, R.G.; Stewart, K.M.; Downey, W.S.; Stevens, N.J. Archaeology, Palaeoenvironment, and Chronology of the Tsodilo Hills White Paintings Rock Shelter, Northwest Kalahari Desert, Botswana. *J. Archaeol. Sci.* **2000**, *27*, 1085–1113. [CrossRef]
3. Lavachery, P. The Holocene Archaeological Sequence of Shum Laka Rock Shelter (Grassfields, Western Cameroon). *Afr. Archaeol. Rev.* **2001**, *18*, 213–247. [CrossRef]
4. Angelucci, D.E.; Boschian, G.; Fontanals, M.; Pedrotti, A.; Vergés, J.M. Shepherds and Karst: The Use of Caves and Rock-Shelters in the Mediterranean Region during the Neolithic. *World Archaeol.* **2009**, *41*, 191–214. [CrossRef]
5. MacDonald, D.H. The Role of Lithic Raw Material Availability and Quality in Determining Tool Kit Size, Tool Function, and Degree of Retouch: A Case Study from Skink Rockshelter (46NI445), West Virginia. In *Lithic Technology*; Cambridge University Press: Cambridge, UK, 2008; pp. 216–232.
6. Högberg, A.; Larsson, L. Lithic Technology and Behavioural Modernity: New Results from the Still Bay Site, Hollow Rock Shelter, Western Cape Province, South Africa. *J. Hum. Evol.* **2011**, *61*, 133–155. [CrossRef] [PubMed]
7. Marciani, G.; Arrighi, S.; Aureli, D.; Spagnolo, V.; Boscato, P.; Ronchitelli, A. Middle Palaeolithic Lithic Tools: Techno-Functional and Use-Wear Analysis of Target Objects from SU 13 at the Oscurusciuto Rock Shelter, Southern Italy. *J. Lithic Stud.* **2018**, *5*. [CrossRef]
8. Abrunhosa, A.; Pereira, T.; Márquez, B.; Baquedano, E.; Arsuaga, J.L.; Pérez-González, A. Understanding Neanderthal Technological Adaptation at Navalmaíllo Rock Shelter (Spain) by Measuring Lithic Raw Materials Performance Variability. *Archaeol. Anthr. Sci.* **2019**, *11*, 5949–5962. [CrossRef]
9. Diez Castillo, A. *Utilización de Los Recursos en la Marina y Montaña Cantábricas: Una Prehistoria Ecológica de los Valles del Deva y Nansa*; AGIRI Arkeologi Kultur Elkartea: Guernica, Spain, 1997.
10. Murray, R.W. Chemical Criteria to Identify the Depositional Environment of Chert: General Principles and Applications. *Sediment. Geol.* **1994**, *90*, 213–232. [CrossRef]
11. Abrajevitch, A. Diagenetic Formation of Bedded Chert: Implications from a Rock Magnetic Study of Siliceous Precursor Sediments. *Earth Planet. Sci. Lett.* **2020**, *533*, 116039. [CrossRef]
12. Adachi, M.; Yamamoto, K.; Sugisaki, R. Hydrothermal Chert and Associated Siliceous Rocks from the Northern Pacific Their Geological Significance as Indication Od Ocean Ridge Activity. *Sediment. Geol.* **1986**, *47*, 125–148. [CrossRef]
13. Chen, D.; Qing, H.; Yan, X.; Li, H. Hydrothermal Venting and Basin Evolution (Devonian, South China): Constraints from Rare Earth Element Geochemistry of Chert. *Sediment. Geol.* **2006**, *183*, 203–216. [CrossRef]
14. Howard, J.L. The Quartzite Problem Revisited. *J. Geol.* **2005**, *113*, 707–713. [CrossRef]
15. Prieto, A.; Yusta, I.; Arrizabalaga, A. Defining and Characterizing Archaeological Quartzite: Sedimentary and Metamorphic Processes in the Lithic Assemblages of El Habario and El Arteu (Cantabrian Mountains, Northern Spain). *Archaeometry* **2019**, *61*, 14–30. [CrossRef]
16. Bertorino, G.; Franceschelli, M.; Luglie, C.; Marchi, M.; Columbu, S. Petrographic Characterisation of Polished Stone Axes from Neolithic Sardinia: Archaeological Implications. *Period. Mineral.* **2002**, *71*, 87–100.
17. Columbu, S.; Garau, A.M.; Lugliè, C. Geochemical Characterisation of Pozzolanic Obsidian Glasses Used in the Ancient Mortars of Nora Roman Theatre (Sardinia, Italy): Provenance of Raw Materials and Historical–Archaeological Implications. *Archaeol. Anthr. Sci.* **2019**, *11*, 2121–2150. [CrossRef]
18. Columbu, S. Petrographic and Geochemical Investigations on the Volcanic Rocks Used in the Punic-Roman Archaeological Site of Nora (Sardinia, Italy). *Environ. Earth Sci.* **2018**, *77*, 577. [CrossRef]
19. Columbu, S.; Antonelli, F.; Sitzia, F. Origin of Roman Worked Stones from St. Saturno Christian Basilica (South Sardinia, Italy). *Mediterr. Archaeol. Archaeom.* **2018**, *18*, 17–36. [CrossRef]
20. Columbu, S.; Palomba, M.; Sitzia, F.; Murgia, M.R. Geochemical, Mineral-Petrographic and Physical-Mechanical Characterization of Stones and Mortars from the Romanesque Saccargia Basilica (Sardinia, Italy) to Define Their Origin and Alteration. *Ital. J. Geosci.* **2018**, *137*, 369–395. [CrossRef]

21. Columbu, S.; Piras, G.; Sitzia, F.; Pagnotta, S.; Raneri, S.; Legnaioli, S.; Palleschi, V.; Lezzerini, M.; Giamello, M. Petrographic and Mineralogical Characterization of Volcanic Rocks and Surface-Depositions on Romanesque Monuments. *Mediterr. Archaeol. Archaeom.* **2018**, *18*, 37–64. [CrossRef]
22. Raneri, S.; Pagnotta, S.; Lezzerini, M.; Legnaioli, S.; Palleschi, V.; S., C.; Neri, N.; Mazzoleni, P.; Raneri, S. Examining the Reactivity of Volcanic Ash in Ancient Mortars by Using a Micro-Chemical Approach. *Mediterr. Archaeol. Archaeom.* **2018**, *18*, 147–157. [CrossRef]
23. Ramacciotti, M.; Gallello, G.; Pastor, A.; Diez Castillo, A.; García Puchol, O. Chert Nucleus and Cortex Characterization for Archaeological Provenance Study Tested in the Prebaetic System Region (Valencian Community, Spain). *Lithic Technol.* **2019**, *44*, 166–180. [CrossRef]
24. Ramacciotti, M.; Rubio, S.; Gallello, G.; Lezzerini, M.; Raneri, S.; Hernandez, E.; Calvo, M.; Columbu, S.; Morales, A.; Pastor, A.; et al. Chemical and Mineralogical Analyses on Stones from Sagunto Castle (Spain). *J. Archaeol. Sci. Rep.* **2019**, *24*, 931–938. [CrossRef]
25. Ramacciotti, M.; Rubio, S.; Gallello, G.; Lezzerini, M.; Columbu, S.; Hernandez, E.; Morales-Rubio, A.; Pastor, A.; de la Guardia, M. Chronological Classification of Ancient Mortars Employing Spectroscopy and Spectrometry Techniques: Sagunto (Valencia, Spain) Case. *J. Spectrosc.* **2018**, *2018*, 9736547. [CrossRef]
26. Ramacciotti, M.; Gallello, G.; Columbu, S.; Fancello, D.; Diez-Castillo, A.; Pastor, A.; Cervera, M.L. Smartphone as an Analytical Tool for Siliceous Artefacts Non-Destructive Characterisation. *STAR Sci. Technol. Archaeol. Res.* **2023**, *in press*.
27. Marquínez, J.; Adrados, L. Geología y Relieve de Los Picos de Europa. *Nat. Cantab.* **2000**, *1*, 3–19.
28. López-Gómez, J.; Martín-González, F.; Heredia, N.; de la Horra, R.; Barrenechea, J.F.; Cadenas, P.; Juncal, M.; Diez, J.B.; Borruel-Abadía, V.; Pedreira, D.; et al. New Lithostratigraphy for the Cantabrian Mountains: A Common Tectono-Stratigraphic Evolution for the Onset of the Alpine Cycle in the W Pyrenean Realm, N Spain. *Earth Sci. Rev.* **2019**, *188*, 249–271. [CrossRef]
29. Herrero-Alonso, D.; Tarriño-Vinagre, A.; Fernández-Martínez, E.; Fuertes-Prieto, N.; Neira-Campos, A. Black Chert and Radiolarite: Knappable Lithic Raw Materials in the Prehistory of the Cantabrian Mountains (North Spain). *Archaeol. Anthr. Sci.* **2021**, *13*, 113. [CrossRef]
30. Bahamonde, J.R.; Vera, C.; Colmenero, J.R. Geometría y Facies Del Márgen Progradante de Una Plataforma Carbonatada Carbonífera (Unidad de Picos de Europa, Zona Cantábrica). *Rev. Soc. Geol. España* **1997**, *10*, 163–181.
31. Rodríguez Fernández, L.R.; Heredia, N. La Estratigrafía Del Carbonífero y La Estructura de La Unidad de Pisuerga-Carrión. NO de España. *Cad. Lab. Xeolóxico Laxe* **1988**, *12*, 207–229.
32. Alonso, J.L.; Marcos, A.; Villa, E.; Súarez, A.; Merino-Tomé, O.A.; Fernández, L.P. Mélanges and Other Types of Block-in-Matrix Formations in the Cantabrian Zone (Variscan Orogen, Northwest Spain): Origin and Significance. *Int. Geol. Rev.* **2014**, *57*, 563–580. [CrossRef]
33. Alonso, V.; González Suárez, J.J. Presencia de Hielo Glaciar En Los Picos de Europa (Cordillera Cantábrica). El Helero de Jou Negro. *Cuatern. Geomorfol.* **1998**, *12*, 35–44.
34. Jiménez-Sanchez, M.; Marquínez, J. Morfología Glaciar En La Cuenca Alta Del Río Nalón, Cordillera Cantábrica. In *Actas I Reunión Nacional de Geomorfología*; Gutierrez, M., Pena, J.L., Lozano, M.V., Eds.; Instituto de Estudios Turolense: Teruel, Spain, 1990; Volume 1, pp. 179–190. ISBN 84-86982-16-2.
35. Flor, G.; Baylòn, J.I. Glaciarismo Cuaternario En Los Puertos de Aliva (Macizo Oriental de Los Picos de Europa, Occidente de Cantabria). *Cuatern. Geomorfol.* **1989**, *3*, 27–34.
36. Farias, P.; Marquínez, J.; González, M. Geomorfología y Origen de La Depresión de Comeya, Picos de Europa, Asturias. In *Actas de la I Reunión Nacional de Geomorfología*; Gutierrez, M., Pena, J.L., Lozano, M.V., Eds.; Instituto de Estudios Turolense: Teruel, Spain, 1990; pp. 91–101, ISBN 84-86982-16-2.
37. Jiménez-Sanchez, M. El Glaciarismo En La Cuenca Alta Del Río Nalón (NO de España): Una Propuesta de Evolución de Los Sistemas Glaciares Cuaternarios En La Cordillera Cantábrica. *Rev. Soc. Geol. España* **1996**, *9*, 157–168.
38. Tarriño-Vinagre, A.; Elorrieta, I.; García-Rojas, M. Flint as Raw Material in Prehistoric Times: Cantabrian Mountain and Western Pyrenees Data. *Quat. Int.* **2015**, *364*, 94–108. [CrossRef]
39. Herrero-Alonso, D.; Tarriño-Vinagre, A.; Neira-Campos, A.; Fuertes-Prieto, N. Chert from the Vegamián Formation: A New Raw-Material Supply Source in the Cantabrian Mountains (NW Spain) during Prehistory. *J. Lithic Stud.* **2016**, *3*, 389–410. [CrossRef]
40. Prieto, A.; Yusta, I.; García-Rojas, M.; Arrizabalaga, A.; Baena Preysler, J. Quartzite Procurement in Conglomerates and Deposits: Geoarchaeological Characterization of Potential Catchment Areas in the Central Part of the Cantabrian Region, Spain. *Geoarchaeology* **2021**, *36*, 490–510. [CrossRef]
41. Diez Castillo, A. El Abrigo de La Calvera (Camaleño, Cantabria). In *Illunzar*; AGIRI Arkeologi Kultur Elkartea: Guernica, Spain, 1997; Volume 3, pp. 81–89.
42. Buosi, C.; Columbu, S.; Ennas, G.; Pittau, P.; Scanu, G.G. Mineralogical, Petrographic, and Physical Investigations on Fossiliferous Middle Jurassic Sandstones from Central Sardinia (Italy) to Define Their Alteration and Experimental Consolidation. *Geoheritage* **2019**, *11*, 729–749. [CrossRef]
43. Columbu, S.; Cruciani, G.; Fancello, D.; Franceschelli, M.; Musumeci, G. Petrophysical Properties of a Granite-Protomylonite-Ultramylonite Sequence: Insight from the Monte Grighini Shear Zone, Central Sardinia, Italy. *Eur. J. Mineral.* **2015**, *27*, 471–486. [CrossRef]

44. Columbu, S.; Mulas, M.; Mundula, F.; Cioni, R. Strategies for Helium Pycnometry Density Measurements of Welded Ignimbritic Rocks. *Measurement* **2021**, *173*, 108640. [CrossRef]
45. Tarriño Vinagre, A.; Duarte Matías, E.; Santamaría Álvarez, D.; Martínez Fernández, L.; Fernández de la Vega Medina, J.; Suárez Ferruelo, P.; Rodríguez Otero, V.; Forcelledo Arena, E.; de la Rasilla Vives, M. El Sílex de Piloña: Caracterización de Una Nueva Fuente de Materia Prima Lítica En La Prehistoria de Asturias. In *F. Javier Fortea Pérez: Universitatis Ovetensis Magister. Estudios en Homenaje*; Ediciones de la Universidad de Oviedo: Oviedo, Spain, 2013; pp. 115–132, ISBN 978-84-8317-983-3.
46. Campos, A.N.; Prieto, N.F.; Alonso, D.H. The Mesolithic with Geometrics South of the 'Picos de Europa' (Northern Iberian Peninsula): The Main Characteristics of the Lithic Industry and Raw Material Procurement. *Quat. Int.* **2016**, *402*, 90–99. [CrossRef]